The College of Engineering
University of Wisconsin-Madison

Wisconsin Electric Machines and Power Electronics Consortium

RESEARCH REPORT
91-29

Input Current Shaping in Brushless DC Motor Drives Utilizing Inverter Current Control

J. Skinner, T.A. Lipo
University of Wisconsin-Madison
1415 Johnson Drive
Madison, WI 53706

WEMPEC

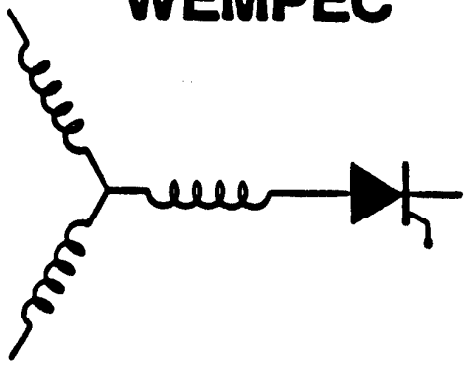

Department of Electrical and Computer Engineering
1415 Johnson Drive
Madison, Wisconsin 53706

Input Current Shaping in Brushless DC Motor Drives Utilizing Inverter Current Control

J. Skinner and T.A. Lipo

University of Wisconsin-Madison, Madison WI 53706, U.S.A.

INTRODUCTION

Typically, electrical power conversion is performed by converting the AC line voltage to DC and then, using a solid-state power converter, converting the DC to the desired voltage and frequency by means of an inverter. Traditionally, at least at low power levels, very little design effort is expended on the rectifier portion of the system. In most cases conversion is accomplished by simply rectifying the AC input and then heavily filtering the resulting waveform with a large capacitor to yield a nearly constant DC level. While this approach is attractive because it is cheap, robust and straightforward, the input current is drawn in narrow pulses since the capacitor voltage drops only slightly between voltage peaks. The problem is particularly severe in units with single phase units where the input power inherently pulsates at twice line frequency.

In this paper it is proposed that the PWM inverter of a conventional brushless DC motor drive be treated as a buck converter. In particular, if the DC link capacitor is simply eliminated then a basic buck configuration current shaper can be realized. In this configuration the inverter switches can be used to control the motor current as before but can also used indirectly to shape the average input current wave shape. In effect the control strategy hinges on the fact that the power to the rectifier pulsates unidirectionally at twice line frequency if the input current is sinusoidal and unity power factor. The current can be made to be sinusoidal and unity input power factor if the output current is controlled to force the output power supplied to the ac machine to pulsate at this same frequency. While this causes the torque to also pulsate at twice line frequency, this 120 Hz pulsation (for a 60 Hz supply) does not result in appreciable speed oscillations in most practical drives due to the system inertial. Since the power input to the dc link filter as well as the output power pulsates at the same 120 Hz pulsation frequency, the energy storage requirement of the dc link filter is not needed and can essentially be eliminated.

This type of strategy is very attractive since current shaping can be achieved with fewer parts than a conventional inverter simply by simply eliminating the link capacitor and by modifying the control strategy. This gain in input current waveshape is obtained at the expense of increased stresses in the inverter switches and a relatively large amount of torque ripple. Because of these tradeoffs this concept is probably most applicable to smaller permanent magnet motor drives where the power switches could be oversized with little cost penalty and where the poor stator current waveform does not cause appreciable extra losses. In addition, this new drive system control strategy would best be applied to a relatively high inertia load where speed is the controlled quantity.

METHODS OF LINE CURRENT SHAPING

Various means of reducing the distortion of the input current of the diode bridge/capacitor AC to DC converter can be divided into the general categories of passive and active. The simplest method of passive input current shaping is to simply insert an inductor between the diode bridge and dc capacitor of the previous circuit, converting it to an inductor-input filter as shown in Fig. 1. The inductance limits the rate of change of current and forces the current to flow for a longer period. In the limiting case, as the inductance becomes very large, the input current becomes a square wave, and the power factor approaches 0.9.

Another type of passive current shaping employs a series resonant input filter as shown in Fig. 2. This circuit can provide a power factor of unity for large values of inductance. The drawbacks of this method are that it is limited to one input frequency and that the resonant components must store a large amount of power.

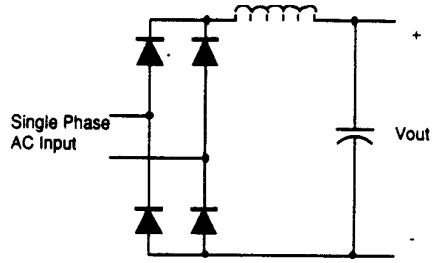

Figure 1 AC to DC Converter with Inductor Input.

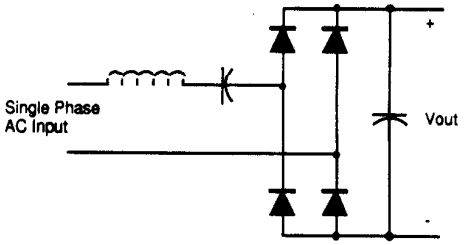

Figure 2 AC to DC Converter with Series Resonant Input.

With the arrival of low cost transistor switches, active methods of current shaping are becoming of increasing importance. Because these methods use high switching frequencies the reactive components can typically be greatly reduced in size. In general, active shapers can be divided into buck-based and boost-based types[1]. Buck-based types have a switch on the input followed by an inductor such that no input current flows when the switch is off (Fig. 3a) whereas boost-based types have the inductor in series with the input, forcing the input current and the inductor current to be the same at all times (Fig. 3b).

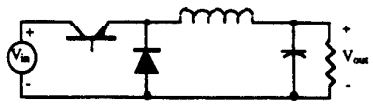

a) Basic Buck Converter

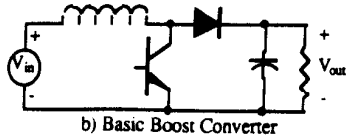

b) Basic Boost Converter

Figure 3 Basic DC/DC Converter Circuits.

Thusfar, boost type converters [3,4] have seen more widespread use as current shapers. In this topology the inductor can be small, limited only by the switching frequency and the allowable ripple current. Inductor current can be continuous or discontinuous. The

input inductor tends to filter the switching frequency from the input current, especially in the continuous current case. In the discontinuous case, a constant duty cycle will result in the peak current of each current pulse being proportional to the instantaneous input voltage. This "automatic", nearly ideal current shaping, simplifies the control system, although some distortion, especially at lower output voltages, is inherent in this method due to the current drawn from the input while the switch is off[2]. The drawback to this method is the high input current ripple, requiring an input filter (as in the buck-based current shapers) and placing higher peak stresses on the circuit components. If the inductor current is continuous then current control can be utilized to give virtually ideal current wave shape.

Typically the wave shape of the input current is derived from the input voltage waveform with the amplitude being controlled by feedback of the output voltage. Freeland [1] shows that this is actually preferable to a pure sinusoidal wave shape since it yields better power factor when the input voltage is distorted. In addition, this method tends to correct any voltage distortion present. This is one of the rare cases when the simplest solution is indeed the best, not only in terms of simplicity, but also in performance.

Similarly, buck-based converters can be operated in either continuous or discontinuous mode. For automatic shaping the inductor current must be discontinuous as before, and this method suffers from distortion introduced by the output voltage affecting the current ramp. The buck converter has another problem that may distort the input current regardless of the control method used: In particular, inductor current cannot be maintained indefinitely when the input voltage is less than the load voltage. This is not a problem when the inductance is so large that the inductor current cannot change significantly over each cycle, but remains difficult for low values of inductance. In general, higher switching frequencies do not offer any benefit in this regard as it is the line frequency that determines the critical value of inductance. For this reason the load voltage must be limited to some small fraction of the peak input for satisfactory input wave shape with a small inductance.

The flyback converter, classified as a buck converter for input current shaping purposes, combines the best features of both the buck and boost shapers and does not suffer from any distortion of the input waveform due to the output voltage when used as an automatic shaper. However, the inductor must store all the energy transferred to the load each switching cycle, making this inductor large and costly. For this reason the flyback topology is not practical at significant power levels.

SELECTED IMPLEMENTATION

Upon examination of the basic single phase fed, dc voltage link PWM inverter it becomes apparent that the basic configuration is simply that of a buck converter, neglecting the multiple devices needed for commutation of the machine. In this configuration the inverter switches used to control the motor current as before are also used to shape the average input current wave shape. Current shaping can be achieved with even fewer parts than a conventional inverter simply by eliminating the DC link capacitor and modifying the control strategy as shown in Fig. 5. The primary objective of this paper is the development of an inverter control strategy for use with a DC brushless motor that has an input current waveform closely resembling the input voltage waveform which can still satisfy the load requirments of the brushless motor. Since the motor used has airgap magnets, it is clear that no rotor currents are induced by the consequent ripple in the stator currents. A secondary objective is to this controller with a minimum of extra parts, especially power switches or large energy storage inductors and capacitors.

Clearly, there are some drawbacks to this method. The top speed of the motor is reduced, all other things being equal, because of the lower average link voltage. Perhaps the most serious limitation is that, due to the moderate inductance of the machine, motor current varies substantially over each input cycle and results in a considerable amount of torque ripple at 120 Hz. The peak currents in the switching devices and motor are substantially higher than the average

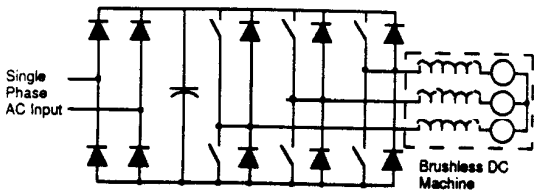

Figure 4 Conventional rectifier fed drive system.

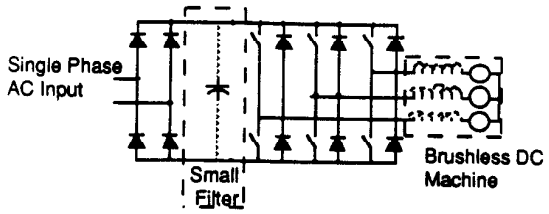

Figure 5 Proposed drive system.

current. Motor current cannot always be maintained near the zero crossing of the line voltage. This results in some unavoidable distortion of the input current in this region. This effect is most noticeable at higher speeds when the back emf of the machine drives the current down more quickly. In order to limit this distortion the back emf can be limited to some fraction of the peak line voltage. Although the currents are distorted, the wave shape is greatly improved over the conventional diode bridge/capacitor input configuration.

Since input current, or more correctly the low frequency components of that current, are of primary importance this need dictates the design of a control system with input current as the inner most loop. This requirement is easily accomplished in a fixed frequency PWM system by integration of the link current while the switch is on. The switch is turned off when the integrated current reaches a value equal to the desired input current integrated over the entire PWM interval. Since the period is fixed and the commanded current is nearly constant over each period the later integration can be reduced to a simple multiplication by the PWM period. This concept is shown in Fig. 6.

Given a means of controlling the input current, a means of controlling the system must now be implemented. Given that the torque of the system varies widely over an input cycle it is most reasonable to develop a speed control loop. A standard PI regulator is used for the speed error and generates the peak value of the input current desired. This quantity is multiplied by the rectified input voltage to generate the desired input current. The complete system is shown in Fig. 7.

As mentioned previously, in some cases motor current cannot always be maintained near the zero crossing of the input voltage. While this presents no major control or stability problems, the input current waveforms are adversely affected. Although the input current is constrained in this manner, some flexibility still remains in choosing the wave shape. The basic control scheme outlined above results in an input current waveform which is basically sinusoidal except for an interval around the zero crossing where it is zero. Due to the load inductance, the current can be maintained for a short time after the input voltage has gone below the back emf. Appendix A contains a more thorough comparison of such a waveform to other possible wave shapes and gives harmonic and THD data for the various waveforms. This control scheme can be deemed nearly optimum in terms of simplicity, low cost, and minimum harmonics.

One difficulty with this inverter arrangement not directly related to the particular control scheme is the possibility of negative link current. If the phase connected to the positive supply is commutated while the lower, controlled switch is off, any motor current will

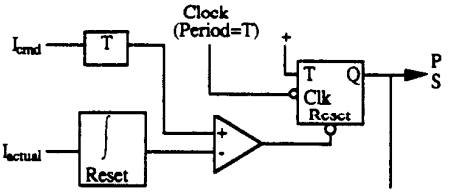

Figure 6 PWM control circuit for averaged input current.

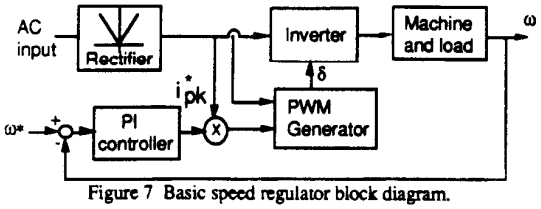

Figure 7 Basic speed regulator block diagram.

appear on the supply link in the negative direction. To prevent overvoltage damage to the switching devices and other components this must be protected against in some manner. In the simulations the commutation of the phases is synchronized with the turn on of the PWM signal. While this minimizes the problem, it does not eliminate it. A small capacitor or transient suppressor must be utilized to limit the voltage of the link as shown in Fig. 5.

SIMULATION RESULTS

The speed control system previously discussed was designed using a classical PI regulator as described earlier. The inertia of the load was large and acted as a dominant pole in the response of the system. The gains were determined experimentally and had to be kept low to minimize the distortion of the input current caused by the speed ripple. It was determined that the system was stable and presented no unusual behavior. Although no direct control of motor current is used, the peak currents were adequately limited by limiting the speed command ramp. A current limit could be utilized to prevent damage to the inverter under fault conditions but it would cause the input current to be highly distorted when active.

The simulations used a 20 kHz PWM frequency and simulated the motor in phase variables. Since the eddy currents in the rotor are considered as negligible, the motor can be modeled very simply by decoupling the phases as accomplished by Demerdash, Nehl, and Maslowski[5] In the decoupled model each phase inductance is equal to one half the open circuit line to line inductance. To simplify the control strategy only two motor phases were energized at any given time. Some limited improvement in input current wave shape and winding and switch utilization might be realized by development of a more sophisticated algorithm that could energize all three phases simultaneously. Although the simulations used a motor with sinusoidal back emf, a motor with trapezoidal back emf could have been used as well.

In general, the inherent torque ripple of the system results in speed ripple that causes distortion of the input current and limits the gain of the feedback loop. Simulation of control system startup with a speed error of 0.5 rad/s is shown in Fig. 8. The response of the system and the ripple in speed and commanded peak input current can readily be seen.

Estimation of the speed ripple was investigated with the intent of canceling the ripple in the feedback signal. An estimate of the speed ripple was developed based on the peak current command and the motor speed. It was assumed that the major component of the ripple was at 120 Hz and both the amplitude and phase of that ripple were measured at various operating points. Various combinations of these variables were fit using polynomial curve fits with the best fit having deviations in amplitude of 20 percent from the actual observed ripple. This estimate utilized a first order fit of the speed, peak current, and peak current divided by speed which is approximately proportional to

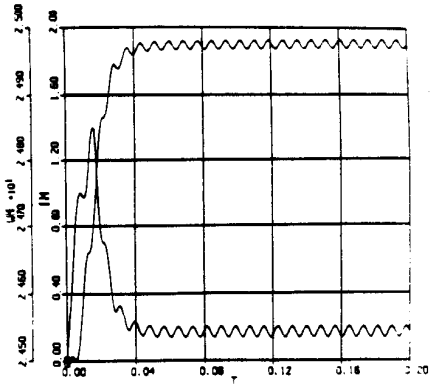

Figure 8 Startup Response of System (No Ripple Cancelation).

load torque. The instantaneous estimated ripple was subtracted from the speed feedback signal. Although the distortion of the system was reduced by this method, the ripple estimate obtained was not as good as had been expected and more work is needed to refine the procedure.

For the purpose of simulation two models were developed. The first used a DC motor model as a load and used continuous, averaged models for the PWM switching and motor parameters. In this way the dynamic performance and low frequency operation could be simulated quickly. A second model included the complete three phase motor and inverter model as well as the actual PWM switching. Comparison of simulations using the two models yielded virtually identical speed loop response.

The low frequency model was used to simulate the system at various operating conditions. The motor and input currents are shown in Fig. 9 for a torque of 2.0 N-m and speeds of 25 and 125 rad/s. The corresponding harmonic content is shown in Fig. 9. It is noted that at high torque and low speed the motor current is continuous and the input current can be controlled at all times. At lower torques and higher speeds the problem of distortion at low input voltage appears.

The power factor, harmonic content, and THD of the input current are also shown. The ratio of back emf to peak line voltage (165 V) and corresponding "blanking" angle can be calculated from the averaged voltage constant of 0.7162 v-s/rad. The spectral content and power factor correlate well with the idealized results given in Appendix A (Table A1).

Torque	2.0 N-m	Torque	2.0 N-m
PF	0.9998	PF	0.9504
Normalized Harmonics		Normalized Harmonics	
3rd	0.01596	3rd	0.2188
5th	0.003185	5th	0.1599
7th	0.001246	7th	0.04024
9th	0.000298	9th	0.05053
THD	0.0163	THD	0.2786

Table 1 Currents at 25 and 125 rad/s Using Results of Simplified Model.

Figure 10 shows the input current waveform of the complete model for a torque of 2.0 N-m at speeds of 25 rad/s and 125 rad/s. The ratios of back emf to peak line voltage are 11% and 54%

respectively. Note the commutation notches and the loss of control about the zero crossing. Some deviations from the low frequency model results are apparent as the current was continuous for that model at the same conditions of Fig. 9.

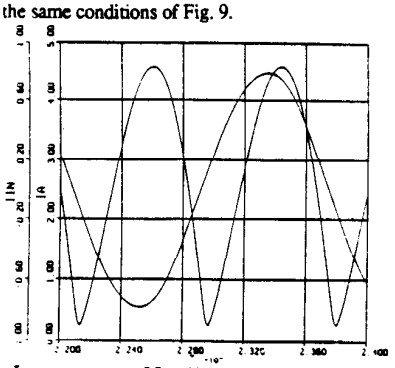

Figure 9a Input current at 25 rad/s using simplified model showing AC input current and DC side current.

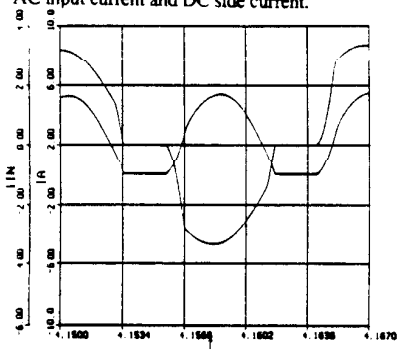

Figure 9b Input current at 125 rad/s using simplified model showing AC input current and DC side current.

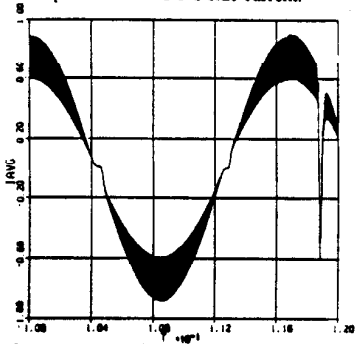

Figure 10a Input current at 25 rad/s using complete model showing AC input current.

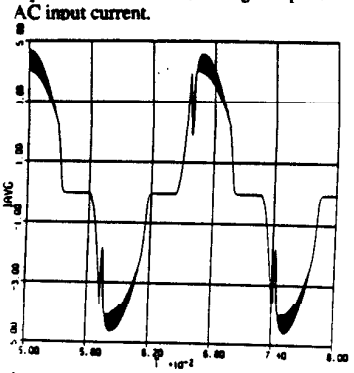

Figure 10b Input current at 125 rad/s using complete model showing AC input Current.

COMPARISON TO BOOST CONVERTER

It is useful to compare the performance and cost of this system to an alternative solution to the problem of power factor correction. The obvious candidate for comparison is a similar inverter but with constant bus voltage fed by a boost converter. The system developed in this research will be referred to as the capacitorless inverter and the boost converter input system as the boost input inverter.

The peak stresses in the various devices occur at the rated speed of 125 rad/s and the rated load of 2.0 N-m and are shown in Table 2. Only the lower switches are used to control the currents; the upper switches are used only for commutation and have the same currents as the motor phases. Currents for the same speed and load can be calculated for the boost input inverter. It is noted that the machine used with the boost input inverter is assumed to be rewound such that the back emf of the machine at full speed is 90% of the bus voltage of 380 volts. This choice allows for maximum utilization of the motor and switches.

Motor speed	124.23 Rad/s
Peak input current (I_{pk})	4.32 A
Load torque	2.0 N-m
RMS phase current	3.475 A
Average phase current	2.498 A
Average diode current	0.5547 A
Average switch current (lower)	3.004 A
Peak motor current	6.323 A

Table 2 Peak Stresses in Capacitorless Inverter and Motor

Perhaps the most difficult aspect of this comparison is the development of a realistic cost differential based on the component stresses. For this reason the comparison has been simplified as much as practical. The boost converter design has been covered in detail in numerous times and will not be detailed here. At present, several companies are introducing integrated circuits that perform the control functions for a power factor correction (PFC) circuit of this type, making implementation straightforward in this case. The data sheet from Micro Linear for their ML4812 PFC IC includes a 200 watt application that was used as a guide in sizing and pricing components for the cost comparison. Several sources[2,3] indicate that the efficiency of the boost PFC stage is typically on the order of 95% while a typical rectifier/capacitor stage without power factor correction is 99%. Rather than simulate this stage these figures have simply been used to calculate losses.

In specifying the filter capacitor it was determined that it would be appropriate to parallel the large electrolytic capacitor (330 mF) with a film capacitor of 3 μF to bypass the switching frequency currents in the electrolytic capacitor. This reduces the RMS current through the electrolytic significantly. In the 'capacitorless' inverter the film capacitor and the input inductor are retained as the input filter required for that topology. The input inductor is a 2 mH device wound on a toroidal core. With this background, the cost comparison of the two systems is shown in Table 3 Only those parts that are different are shown. The prices shown are 10 thousand piece prices.

For the loss determination, Table 4, the switching device chosen for the capacitorless inverter was a 10N25, a 10 ampere, 250 volt device with an on-resistance of 0.45 ohms. The device used in the boost input inverter was a 2N50, a 2 ampere, 500 volt device with a 4 ohm on-resistance. The switching device losses calculated were increased by 50 percent to account for the increase in on resistance due to operation at temperatures above the specified 25 degrees Centigrade.

CONCLUSIONS

It has been shown that a significant improvement in input current wave shape can be obtained by elimination of the link capacitor and proper modulation of the inverter switches. This gain is obtained at the expense of increased stresses in the inverter switches and a large amount of torque ripple. Because of these tradeoffs this concept is

Cost Comparison		
	Capacitorless Inverter	Boost Input Inverter
Filter Capacitor (330uF)	0.00	2.28
Boost Switch	0.00	1.96
Boost Diode	0.00	1.01
ML4812 PFC IC	0.00	3.80
Inverter Switches (6 each)	11.16	4.50
Total Cost	$11.16	$13.55

Table 3 Cost Comparison of Capacitorless Inverter vs. Boost Input Converter.

Loss Comparison		
	Capacitorless Inverter	Boost Input Inverter
Losses in Switches	14.8	6.2
Losses in Motor	18.1	11.7
Losses in Rectifier	2.0	10.0
Total Losses	34.9 W	27.9 W

Table 4 Loss Comparison of Capacitorless Inverter vs. Boost Input Converter.

probably most applicable to smaller motor drives where the power switches could be oversized with little cost penalty. In addition, the drive system would need to be applied to a relatively high inertia load where speed is the controlled quantity.

Primarily because of the high torque ripple, this drive system will not always be well suited to general purpose applications. In this case the boost input inverter provides a suitable solution to the problem of power factor correction.

Several improvements in the control algorithm are possible. A method of gradual commutation of the machine would prevent notches in the input line current. A simple way of accomplishing this would be to phase in the new winding gradually once the commutation point is reached. One way of doing this would be to estimate the current in the new winding for the PWM cycle and switch on the previous winding long enough to compensate for any deficiency. This would result in the most rapid transfer of current possible but require a moderate amount of computation and produce slight distortions of the input current due to errors in the model parameters. A simpler scheme would be to simply turn on both the new and previous phase and turn both off when sufficient current for that cycle is obtained as is currently done. The new phase would be turned on at the start of each PWM cycle; the previous phase would be turned on after some delay. This delay would be quickly increased from zero to the full PWM period at a rate that would keep the duty cycle of the new phase as close to 100% as practical.

Some method of eliminating the distortion around the zero crossings of the line voltage is desirable. Complete elimination of this distortion does not seem possible without increasing the number of phases of the machine or using some additional energy storage element. Since the energy storage required during this time is low it may be practical to add small reactive components to this end. Additional thought needs to be given to possible topologies. A circuit with a link capacitor slightly larger than the filter capacitor used in the capacitorless inverter might be used in combination with a boost input that only operated near zero input voltage. Large voltage ripple would be allowed on the DC link but it would always be maintained higher than the back emf of the machine.

REFERENCES

1. Freeland, S.D.,"Input-Current Shaping for Single-Phase AC-DC Power Converters," Ph.D. Thesis, California Inst. of Technology, July, 1988.
2. Chambers, D. and Wang, D.,"Dynamic Power Factor Correction in Capacitor Input Off Line Converters," Proceedings of POWERCON 6, May 2-4, 1979.
3. Mohan, N., et. al., "Sinusoidal Line Current Rectification with a 100 kHz B-SIT Step-Up Converter," IEEE Power Electronics Specialists Conference Record, 1984.
4. Liu, K.H., and Lin, Y.-L., "Current Waveform Distortion in Power Factor Correction Circuits Employing Discontinuous-Mode Boost Converters," IEEE Power Electronics Specialists Conference, 1989.
5. Demerdash, N.A., Nehl, T.W., and Maslowski, E.,"Dynamic Modeling of Brushless DC Motors In Electrical Propulsion and Electromechanical Actuation by Digital Techniques," Conf. Record of IEEE Industry Applications Society, 1980.

APPENDIX A

Harmonic Analysis of Truncated Sine Waveforms

This section details an investigation of various possible input current waveforms with the desire to minimize the total harmonic distortion (THD) and maximize the power factor. The basic constraint on the analysis is that the current waveform must be zero around the zero crossing of the input voltage. This is due to the fact that the current cannot always be maintained when the back emf of the machine is greater than the input voltage. The waveform actually used for the line side current controller is that of Fig. A2 with symmetrical 'blanking' or zero current around the voltage zero crossing. The harmonic amplitudes for all the tables are normalized to a unity amplitude fundamental.

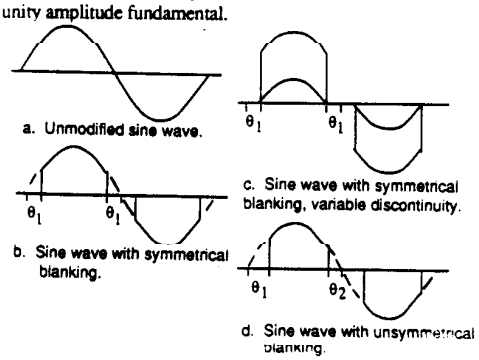

Fig. A1 Possible Input Current Waveforms.

Theta	Fund	3rd	5th	THD
0	1.00	0.00	0.00	0.00
0.314	0.987	0.036	0.051	0.105
0.628	0.903	0.232	0.173	0.315
0.942	0.703	0.564	0.044	0.630
1.257	0.387	0.874	0.652	1.209

Table A1 Spectrum and Total Harmonic Distortion Corresponding to Fig. A1(b) (Method Implemented).

Offset	Fund	3rd	5th	THD
-0.8	1.383	0.100	0.163	0.238
-0.4	1.163	0.119	0.156	0.236
0.0	0.942	0.146	0.146	0.236
0.4	0.722	0.191	0.130	0.247
0.8	0.501	0.275	0.099	0.296

Table A2 Spectrum and Total Harmonic Distortion Corresponding to Fig. A1(c).

Theta	Fund	3rd	5th	THD
0.00	0.923	0.172	0.129	0.247
0.157	0.921	0.176	0.137	0.255
0.314	0.912	0.196	0.158	0.280
0.471	0.893	0.242	0.173	0.324
0.707	0.842	0.348	0.152	0.417

Table A3 Spectrum and Total Harmonic Distortion Corresponding to Fig. A1(d).